Molecular Medicine 7(9): 590–597, 2001

Original Articles

Relationship of the K-ras/c-mos Expression Patterns With Angiogenesis in Non-Small Cell Lung Carcinomas

Panayotis Zacharatos,[1] Athanassios Kotsinas,[1] Petros Tsantoulis,[1] Kostas Evangelou,[1] Dimitris Kletsas,[2] Panayiotis J. Asimacopoulos,[3] Ipatia Doussis-Anagnostopoulou,[1] Francesco Pezzella,[4] Kevin Gatter,[4] Athanasios G. Papavassiliou,[5] Christos Kittas,[1] and Vassilis G. Gorgoulis[1]

[1]Department of Histology and Embryology, School of Medicine, University of Athens, Athens, Greece
[2]Laboratory of Cell Proliferation and Ageing, Institute of Biology, NCSR "Demokritos," Athens, Greece
[3]Department of Cardiac Surgery, School of Medicine, University of Athens, Athens, Greece
[4]Nuffield Department of Clinical Laboratory Sciences, John Radcliffe Hospital, Oxford, United Kingdom
[5]Department of Biochemistry, School of Medicine, University of Patras, Patras, Greece

Contributed by A.G. Papavassiliou. Accepted June 3, 2001

Abstract

Background: Neo-angiogenesis is an acquired capability vital for a tumor to grow and metastasize. Evidence has shown that the mitogen-activated protein (MAP) kinase pathway is involved in this process. Alterations of K-ras and c-mos, two pivotal components of this pathway, have been implicated in non-small cell lung carcinogenesis. In the present report, we examine, in a series of non-small cell lung carcinomas (NSCLCs), the status of K-ras and c-mos oncoproteins in correlation with the tumor neo-angiogenesis state and the major angiogenic factor, vascular endothelial growth factor (VEGF).

Materials and Methods: c-mos and p-ERK1/2 status was evaluated immunohistochemically in a total of 65 NSCLCs, whereas the presence of K-*ras* mutations was examined by reverse transcriptase-polymerase chain reaction (RT-PCR) restriction fragment length polymorphism (RFLP) in available matched normal tumor material from 56 cases. Microvessel density (MVD) was estimated by immunodetection of CD_{31} endothelial marker, and VEGF expression was assessed by immunohistochemistry. All possible associations were examined by a series of statistical methods.

Results: Expression of oncogenic activated K-ras and c-mos overexpression was observed in 12 of 49 (25%) and in 16 of 61 (26%) informative cases, respectively. Only 1 of the 25 deregulated for K-ras or c-mos cases exhibited both alterations, suggesting a mutually exclusive relationship between activated K-ras and c-mos overexpression ($p = 0.074$) in a subset of NSCLCs. In these cases, the MAPK kinase kinase/MEK/ERK pathway was found to be activated. MVD and VEGF expression were 36.9 ± 10.6 mv/mm^2 and 73.1 ± 20.0%, respectively. The most intriguing finding was that the [K-ras(No)/c-mos(P)] profile was significantly associated with low MVD levels compared to normal cases ($p = 0.004$); by contrast, no correlation was found between the other K-ras/c-mos patterns and MVD. Furthermore, the former group exhibited the lowest VEGF levels.

Conclusions: The mutually exclusive relationship between mutated K-*ras* and c-mos overexpression in a subset of NSCLCs implies a common signal transduction pathway in lung carcinogenesis. The effect of this pathway on NSCLC neo-angiogenesis seems to depend upon the status of c-mos, which acts as a molecular "switch," possibly exerting a negative selective pressure on tumor progression.

Introduction

A vascular network is vital for a tumor to grow beyond a critical size and metastasize (1). Angiogenesis is a precisely regulated process, whereby many factors are implicated in a fine-tuned mechanism for the tissues to gain the appropriate blood supply for their survival (2). According to this scenario there are two major categories of modulators of angiogenesis: activators (e.g., VEGF-A, [angiopoietin 1] Ang1, basic fibroblast growth factor, transforming growth factor-α[TGF-α], hepatocyte growth factor, and tumor necrosis factor-α[TNF-α]), and inhibitors (e.g., thrombospondin-1, Ang2, angiostatin, and endostatin). The balance between these groups of factors determines the angiogenic potential (2,3). Under normal conditions, the angiogenic switch is in the "off" state

Address correspondence and reprint requests to: Athanasios G. Papavassiliou, MD, PhD and Vassilis G. Gorgoulis, MD, 53 Antaiou Str., Lamprini, Ano Patissia GR-11146 Athens, Greece. Phone/fax: ++30-1-6535894 or ++30-61-996110; e-mail: papavas@med. upatras.gr or histoclub@ath.forthnet.gr

and leads to a vascular quiescence. Otherwise, when the angiogenic switch is "on," the balance is tipped in favor of angiogenesis (3).

Among these factors, the members of the VEGF family are specific for the vascular endothelium with crucial roles in the angiogenic process (4). VEGF acts on vascular epithelial cells as a mitogenic and motogenic factor, promoting the sprouting and formation of the new vessel-like structures (3,4). Its expression is induced in tumor cells by hypoxia, cytokines, and growth factors such as platelet-derived growth factor (PDGF) and transforming growth factor-β(TGF-β) (5). Recently, it has been found that VEGF expression in tumor cells is stimulated by the Raf/MEK/ERK MAP kinase cascade components src (6), v-raf and v-H-ras (7), K-ras, and MEK-1 (8, and references therein).

Ras proteins comprise a group of membrane-bound GTPases that play a pivotal role in cellular growth and differentiation through signal transduction pathways activated by cell-surface receptors (9). The Ras-dependent signal is transmitted via three effector pathways: the Raf/MEK/ERK (10,11), the phosphatidylinositol 3-kinase (PI3K) (12), and the Ral-GDS/Ral GTPase (13). As a consequence, "second messengers" such as type D phospholipase and Akt/PKB (14,15) and a gamut of transcription factors including Elk-1, Ets-2, CCAAT-enhancer binding protein, activator protein-1, and SMADS (16–19), are activated. In many cancers oncogenic activation of Ras protein is exerted by mutational amino acid substitutions at residues 12, 13, or 61 (20).

C-mos is an upstream activator of the MAPK pathway with serine-threonine kinase activity that activates MAPK kinase (MAPKK) (21). The role of c-mos is well established in oocyte maturation, where it is involved in oocyte arrest at metaphase II by stabilizing the maturation-promoting factor, and in the asymmetric division of the oocyte and the production of the first polar body by modulating the formation and orientation of the meiotic spindle (22). On the other hand, very little is known about its expression and functions in human somatic cells (23), even though its expression induces oncogenic transformation (22). C-mos causes meiotic-like modifications in M phase that lead to the production of binucleated cells and may indicate a novel mechanism of chromosomal instability (24). However, c-mos tumorigenic ability is mainly attributed to its mitogenic function as a stimulator of the MAPK pathway and the consequent activation of many downstream effectors including c-fos, c-jun, c-myc, S6 kinase II, and Elk-1 (25 and references therein). Among them, c-fos has been suggested to be the key molecule for the c-mos–mediated cellular transformation (26). However, the observed deregulation of certain cyclins (D, E, and A), cyclin-dependent kinases ($p33^{cdk2}$ and $p43^{cdk2}$), and S phase-specific E2F complexes in serum-starved v-mos–transformed cells adds a further complexity to the situation (27,28).

Mounting evidence suggests that the MAPKK/MEK/ERK pathway may be involved in tumor neo-angiogenesis (6–8). However, the data concerning the implication of defects of this pathway in non-small cell lung carcinoma (NSCLC) angiogenesis are limited and conflicting (29,30). In the present study, we investigated, in a series of NSCLCs, the relationship between aberrations of the MAPK components, K-ras and c-mos, and tumor neo-angiogenesis. To the best of our knowledge, this is the first report that addresses this issue.

Materials and Methods

Tissue Samples

A panel of 65 NSCLCs, consisting of 29 adenocarcinomas, 31 squamous cell carcinomas, and 5 undifferentiated large carcinomas, was analyzed immunohistochemically for c-mos, p-ERK1/2, VEGF, and neo-angiogenesis status. In 56 of these cases, frozen material and adjacent normal lung tissue was available for K-ras mutation analysis. These tumors were classified according to World Health Organization (WHO) criteria and Tumor-Nodes-Metastases (TNM) system, and a part of them has been previously employed in the study of c-mos status in NSCLCs (31) (Table 1).

Immunohistochemistry

Antibodies For immunohistochemical analysis the following antibodies (Abs) were used: P-19 (class, IgG goat polyclonal; epitope, C-terminus of human c-mos) (Santa Cruz Bioanalytica, Athens, Greece), p-ERK/E-4 (class, IgG2a mouse monoclonal; epitope corresponding to the amino acid sequence containing the phosphorylated Tyr 204 of ERK1/2) (Santa Cruz Bioanalytica), JC/70A (class IgG1, mouse monoclonal; epitope, CD_{31} endothelial marker) (Dako, Kalifronas, Greece), C-1 (class IgG2a, mouse monoclonal; epitope, residues 1-140 of VEGF) (Santa Cruz Bioanalytica).

Method Immuniohistochemical analysis was performed using an indirect streptavidin-biotin-peroxidase method, as previously described (31,32).

Controls The human cervical cell line ME180 and the appropriate control peptide (Santa Cruz Bioanalytica) were used as positive controls for c-mos expression, while the DB lymphoma c-mos negative cell line was used as a negative control (31 and references therein). The specificity of E-4 anti p-ERK antibody was tested by preincubating the latter with the appropriate control peptide (Santa Cruz Bioanalytica). Elimination of the staining verified p-ERK specificity. For CD31 analysis, staining of vessel endothelial cells in the surrounding normal tissue was considered as positive control. As positive controls for VEGF analysis, normal kidney tissue sections recommended by the manufacturer were used.

Table 1. Summary of clinicopathological features, c-mos and K-ras mutation status, MVD, and VEGF expression

c-mos status (normal-tumor tissue comparison)						
Immunohistochemical evaluation (IHC)	P:	14	N:	38		
K-ras mutation status						
Codon 12	P:	8	N:	44		
Codon 13	P:	5	N:	47		
MVD status	M (*n*):	36.9 (65)	SD:	10.6		
VEGF status	M (*n*):	73.1 (65)	SD:	20.0		
Histology	ADCs:	29	SCCs:	31	UL:	5
Lymph node invasion	Yes:	35	No:	30		
Tumor stage	I:	27	II:	20	III:	18

Abbreviations: M, mean value; SD, standard deviation; *n*, number of informative samples; P, positive; N, negative; OE, overexpression; NE, normal expression; Ad, adenocarcinoma; Sq, squamous cell carcinoma; UL, undifferentiated large carcinoma.

Furthermore, in each set of immunoreactions, antibody of the corresponding IgG fraction, but of unrelated specificity, was used as a negative control.

Evaluation

c-mos Cytoplasmic and membranous immunoreactivity was considered to be evidence of c-mos expression. As we have previously described, nuclear staining in the presence of cytoplasmic and/or membranous reactivity was also evaluated as specific, whereas sole nuclear staining was disregarded (31, 32). Immunohistochemistry was evaluated by examining all discreet areas of each tumor specimen. Tumors were considered c-mos positive when more than 30% of the tumor cells were stained; otherwise, they were scored as negative. The criteria were assessed in a recent study showing that carcinomas in which >30% cells exhibit immunoreactivity, are associated with increased *c-mos* mRNA levels (31).

p-ERK1/2 Tumor cells were evaluated as positive when staining was mainly nuclear because activated ERK translocates to the nucleus (31 and references therein).

CD31 Hematoxylin-eosin staining was used to detect invasive areas of the tumor. In immunostained tissues, we defined microvessels as any single brown-staining endothelial cell or aligned clusters of endothelial cells, with or without a formed lumen, separated from adjacent microvessels, tumor cells, and other connective tissue material; plasma cells and T-cell subsets, which similarly stain positive for CD31, were clearly identified by their typical morphology. We note here that other groups exclude single immunohistochemically stained cells claiming, on one hand, that a lumen is necessary for them to be classified as vessels and on the other that single immunostained cells may not be of vascular origin.

VEGF Tumor cells were evaluated as positive when cytoplasmic staining was observed. The percentage of positive cells was counted. Evaluations were performed by three independent observers (P.Z., C.K., V.G.), and interobserver variability was minimal ($p < 0.01$).

RNA Extraction and cDNA Preparation

Cancerous material with more than 90% tumor cells was used for RNA extraction, because microdissection is not suitable for RNA handling methods. RNA was extracted with Trizol reagent (Life Technologies, AntiSel, Athens, Greece) according to the manufacturer's instructions. Two micrograms of total RNA were reverse-transcribed with oligo-dT (NEB, Bio-Line, Athens, Greece) and 200 U Moloney murine leukemia virus reverse transcriptase (Life Technologies, Anti-Sel), according to the supplier's instructions.

K-ras PCR-RFLP Mutation Detection

Codons 12 and 13 of K-ras were screened for mutations in our database. Briefly, BstNI artificial restriction fragment length polymorphic (RFLP) sites for detection of codon 12 mutations were introduced by nucleotide substitution after polymerase chain reaction (PCR) amplification of cDNA transcripts (33). The most common mutation at codon 13 (Gly to Asp) was detected by employing a naturally occurring RFLP (33). The cell lines SW480 (human colon carcinoma) and MDA-MB231 (human breast cancer) carry K-ras mutations at codons 12 and 13, respectively, and were used as positive controls for K-ras mutation analysis (33).

Statistical Analysis

The possible associations between K-*ras* and c-mos status independently, and (K-*ras*/c-mos) patterns with MVD, VEGF status, and clinicopathologic parameters were assessed with *t*-test, the nonparametric Kruskal-Wallis, and Pearson's chi-square tests. Moreover, analysis of variance (ANOVA) was used to evaluate more specifically the possible association between MVD and (K-*ras*/c-mos) patterns. Finally, Spearman bivariate analysis was performed to

examine a possible correlation between MVD and VEGF expression. Analysis was performed with the SPSS10 statistical package. The statistical difference was considered significant when $p < 0.05$.

Results

K-ras, c-mos, and p-ERK1/2 Status: Relationship With Tumor Clinicopathologic Features

Oncogenic activated K-ras [K-ras(A)] (Fig. 1) and c-mos overexpression [c-mos(P)] (Fig. 2) was found in 12 of 49 (25%) and in 16 of 61 (26%) informative cases, respectively (Table 1). Among the 25 samples informative for both K-ras and c-mos status, alterations in K-ras or c-mos were observed in 11 and 13 cases, respectively, and only one case harbored both K-ras mutation and c-mos overexpression. In the latter cases, the MAPK/MEK/ERK pathway was found activated as evaluated by the p-ERK nuclear immunostaining. These observations indicate a mutually exclusive relationship between the presence of K-ras(A) and c-mos(P) in a subset of NSCLCs, which was further supported by a statistical trend ($p = 0.074$, by Pearson's χ^2 test; group categorization in Table 2).

No correlation was found between K-ras and c-mos status and clinicopathologic features (Table 3).

Estimation of MVD in Tumor Areas: Relationship With VEGF Status and Clinicopathologic Parameters of the Patients

MVD ranged from 14–62 microvessels per square millimeter (mv/mm^2), with a mean value of 36.9 $\pm$ 10.6 mv/mm^2 (Table 1 and Fig. 3). No correlation was found between MVD and any of the clinicopathologic features examined (e.g., histology, lymph node invasion, and tumor stage) (Table 3).

VEGF expression varied from 30–100% (mean 73.1 $\pm$ 20.0%) (Table 1 and Fig. 4). No statistically significant association was found between VEGF estimation and any of the clinicopathologic parameters was found (Table 3). MVD positively correlates with VEGF expression ($r = .204$), but this association does not reach significance ($p = 0.106$, by Spearman test).

Fig. 1. Representative results from K-ras mutation (codon 12) analysis. M, 100-bp ladder; lanes 1 and 4, undigested PCR products (357 bps); lanes 2 and 3, PCR products digested with BstNI from cases 44 and 45 harboring K-ras mutation (335 bps); lanes 5 and 6, PCR products digested with BstNI from tumor samples without K-ras mutation (cases 10 and 11); lane 7, negative control.

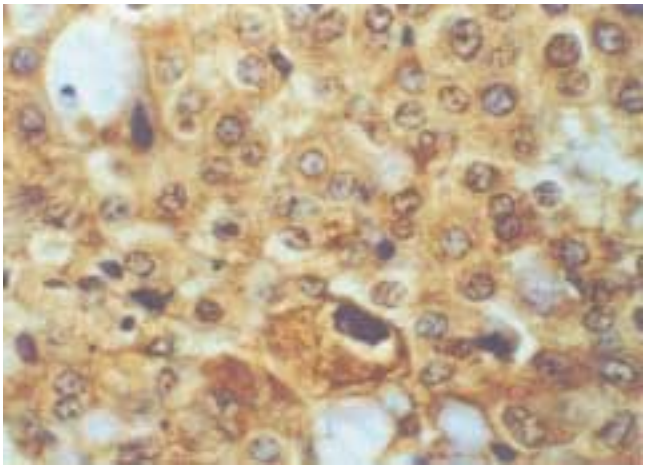

Fig. 2. Lung adenocarcinoma (case 22) with c-mos overexpression. Streptavidin-biotin peroxidase technique with «P19» anti–c-mos antibody (see Methods) and hematoxylin counterstain (original magnification ×630).

Relationship of K-ras and c-mos Status With MVD and VEGF Expression

K-ras mutational activation was not statistically associated with MVD or VEGF expression (Table 2). However, on closer inspection, samples without K-ras mutations [K-ras(No)] exhibited a larger variance in MVD (variance = 124.1) compared to those with activated K-ras (variance = 22.7), suggesting a more heterogeneous group (Fig. 5A) ($p = 0.03$, by F-test).

An interesting finding was that cases with c-mos overexpression appeared to have lower MVD than those with normal c-mos status [c-mos(N)] ($p = 0.003$, by *t*-test) (Table 2 and Fig. 5B). Moreover, in the former group with c-mos overexpression, VEGF expression was found to be lower than that observed in the latter group ($p = 0.045$ by Kruskal-Wallis test) (Table 2).

Relationship of K-ras/c-mos Patterns With MVD, VEGF Expression, and Clinicopathologic Features

Because both K-ras and c-mos are activators of the MAPK pathway, samples were divided into two groups based on the complete absence (No) or presence of at least one aberration (Ab) in the aforementioned molecules. Statistical analysis revealed that the (Ab) group [K-ras–c-mos(Ab)] had lower MVD than that of the (No) one [K-ras–c-mos(No)] ($p = 0.012$, by *t*-test). However, the levels of significance are lower than that of the association between c-mos status and MVD, thus excluding a putative synergistic effect of K-ras and c-mos on MVD (Table 2).

Cases were further categorized into three groups according to K-ras and c-mos status: *(1)* K-ras(No)/c-mos(N), *(2)* K-ras(No)/c-mos(P), and *(3)* K-ras(A)/c-mos(N) (the one specimen with concomitant alterations was excluded from the analysis). Bonferroni analysis revealed that only the K-ras(No)/c-mos(P)

Table 2. Association between K-ras and c-mos, K-ras-c-mos and K-ras/c-mos patterns, and MVD and VEGF

Alteration (number of cases)		MVD (microvessels/mm^2) Mean	StDev	p	VEGF (%) Mean	StDev	p^a
K-ras	No (37)	37.6	11.1	0.801[b]	71.7	21.7	0.801
	A (12)	38.0	4.8		73.4	20.4	
c-mos	N (45)	39.0	9.8	0.003[c]	77.4	16.8	0.045
	P (16)	29.9	10.8		63.4	24.5	
K-ras-c-mos[d]	No (24)	40.7	10.8	0.012[c]	76.9	17.4	0.168
	Ab (25)	33.4	9.6		67.5	23.2	
K-ras/c-mos[e]	No/N (24)	40.7	10.8	0.004[f]	76.9	17.4	0.157
	A/N (11)	38.0	5.2		75.9	19.3	
	No/P (13)	29.3	10.9		62.3	25.0	

[a]Kruskal-Wallis test.
[b]Kruskal-Wallis test; $p = 0.03$ by F-test.
[c]*t*-test
[d]Categorization based on the complete absence or presence of at least one aberration in K-ras or c-mos (see Results section 4).
[e]Categorization into groups according to K-ras and c-mos status (see Results section 4).
[f]ANOVA, $p = 0.003$ between No/P and No/N patterns and $p = 1.000$ between A/N and No/N, by Bonferroni analysis.
A, activated; No, normal; N, negative; P, positive; Ab, aberrant.

pattern was statistically associated with lower MVD, as compared to the normal status K-ras(No)/c-mos (N) ($p = 0.003$) (Table 2 and Fig. 6A). Moreover, Kruskal-Wallis analysis did not reveal any association between the examined patterns and VEGF expression (Table 2 and Fig. 6B).

Table 3. Association between clinicopathologic features and K-ras, c-mos, K-ras–c-mos, K-ras/c-mos, MVD, and VEGF

Status	Histology p	LN p	Stage p
MVD (microvessels/mm^2)	0.850[a]	0.894[a]	0.264[b]
VEGF	0.278[c]	0.315[c]	0.742[c]
K-ras	0.212[d]	0.873[d]	0.980[d]
c-mos	0.752[d]	0.532[d]	0.085[d]
K-ras–c-mos[e]	0.562[d]	0.571[d]	0.265[d]
K-ras/c-mos[f]	0.855[d]	0.882[d]	0.339[d]

[a]*t*-test analysis.
[b]ANOVA.
[c]Kruskal-Wallis analysis.
[d]Pearson's chi-square analysis.
[e]Categorization based on the complete absence or presence of at least one aberration in K-ras or c-mos (see Results section 4).
[f]Categorization into groups according to K-ras and c-mos status (see Results section 4).

No correlation was found between K-ras–c-mos or K-ras/c-mos patterns and clinicopathologic features (Table 3).

Discussion

A discrete critical step for tumor development is to set the angiogenic switch to the "on" state (34). Although deregulation of oncogenes is implicated in the release of cells from controlled proliferation, programmed cell death, migration, and adhesion, little

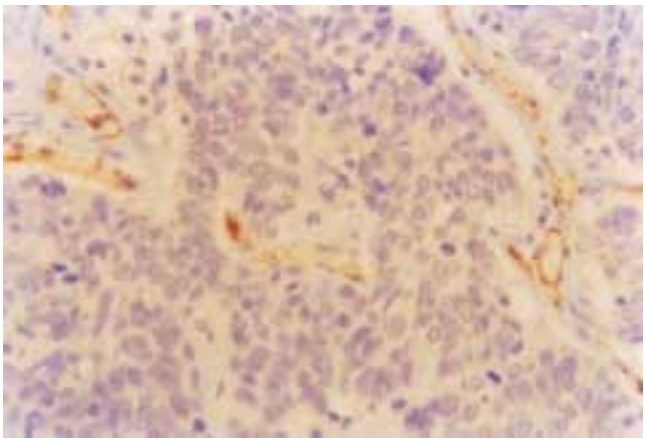

Fig. 3. Squamous cell lung carcinoma (case 28) with CD31 immunoreactivity (38%), representative immunohistochemical result. Streptavidin–biotin peroxidase technique with "JC/70A" anti-CD_{31} antibody (see Methods) and hematoxylin counterstain (original magnification ×400).

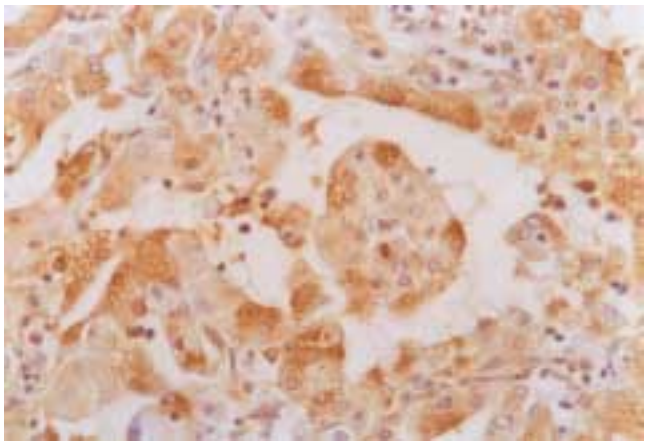

Fig. 4. Lung adenocarcinoma (case 50) with VEGF immunostaining (65%), representative immunohistochemical result. Streptavidin–biotin peroxidase technique with "C-1" anti-VEGF antibody (see Methods) and hematoxylin counterstain (original magnification ×400).

is known about their involvement in tumor angiogenesis (8,34,35). Aberrant expression of oncogenic components of the MAPKK/MEK/ERK pathway, is known to be implicated in NSCL carcinogenesis (11,20,31,32). Limited data are available regarding the involvement of molecules participating in this signaling cascade in tumor neo-angiogenesis, as well as their role in the regulation of the pivotal angiogenic factor VEGF (7,8,29,30). In the present study, we investigated the relationship between alterations of the MAPK pathway components, K-ras and c-mos, with the angiogenic status in a series of NSCLCs.

Examining the status of K-ras and c-mos, we observed that in almost half of the cases, analyzed for both molecules, a mutually exclusive relationship exists between mutationally activated K-ras and overexpressed c-mos. This finding suggests that K-ras and c-mos participate in the same MEK/ERK cascade in a subset of NSCLCs. This notion is further strengthened by the fact that all these cases exhibited nuclear immunoreactivity for activated ERK1/2, as previously demonstrated in our database (31).

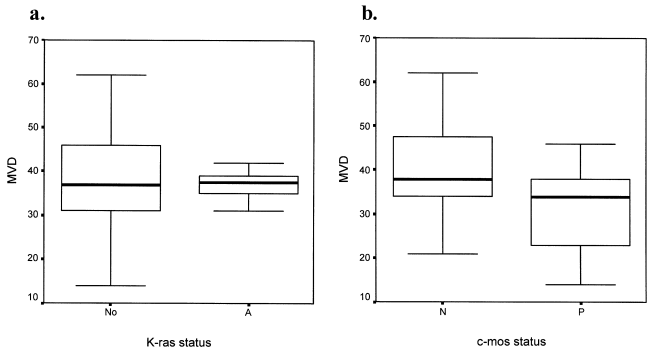

Fig. 5. MVD association. Box plots representing the MVD association with **(A)** K-ras status and **(B)** c-mos status.

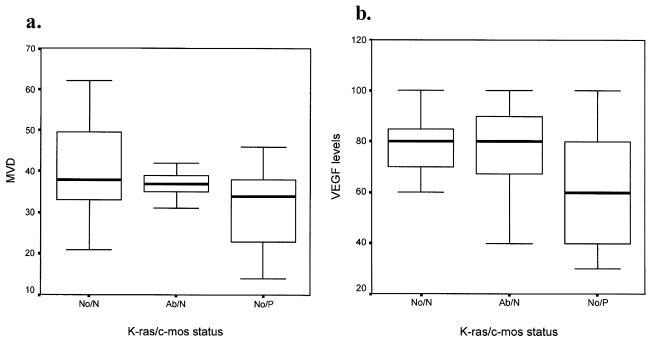

Fig. 6. K-ras/c-mos patterns. Box plots representing the MVD **(A)** and VEGF expression **(B)** of K-ras/c-mos patterns.

Our analysis concerning the relationship between K-ras/c-mos patterns and MVD status revealed several intriguing findings. The carcinomas with the K-ras(No)/c-mos(P) profile exhibited a significantly lower MVD compared to cases with normal K-ras/c-mos pattern ($p = 0.004$, Table 2), whereas the latter profile demonstrated similar MVD values with the K-ras(A)/c-mos(N) one. A question arising from these observations is how do they fit in the currently proposed angiogenesis model (2,36).

According to this model, the following steps are required for angiogenesis: *(1)* proteolytic degradation of the parental vessel membrane and surrounding matrix, *(2)* migration of endothelial cells, *(3)* proliferation of endothelial cells, *(4)* formation of capillary tubes, and *(5)* stabilization of vessels by recruiting periendothelial cells (3,36). The role of VEGF in these steps is vital for the maturation and stabilization of the newly formed vessels, because its absence leads to vessel regression (36). Furthermore, an overwhelming body of evidence implicates members of the MAP kinase kinase/MEK/ERK module in these processes (6–8,37–39). In light of these considerations, our results concerning the relationship between the K-ras/c-mos patterns and MVD have complicated the issue.

One possible explanation is that the K-ras(No)/c-mos(P) pattern is related to vessel regression, which acts in a particular stage of tumor development as a negative selective-pressure mechanism, by creating a hypoxic environment. In accordance with this hypothesis, the K-ras(No)/c-mos(P) carcinomas exhibited the lowest VEGF levels (Table 2, Fig. 6B). Additionally, we have recently observed at the ultrastructural level disruption of the endothelium integrity and absence of the tunica externa in vessels next to c-mos–positive tumor cells (data not shown). However, how can the higher MVD and VEGF levels in the other K-ras/c-mos patterns be explained, in as much as K-ras and c-mos act in the same pathway? The most likely answer lies on the effect K-ras and c-mos exert on VEGF expression or other angiogenic factors. It should be mentioned to this end that VEGF is triggered by a variety of growth factor–regulated

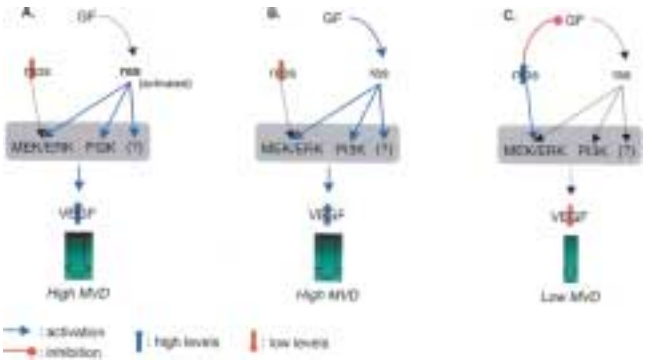

Fig. 7. Hypothetical model describing the effects of the K-ras/c-mos patterns on tumor neo-angiogenesis. Cases with mutated K-ras and/or stimulated growth factor (GF) autocrine loops (**A** and **B,** respectively) activate signaling cascades, such as MEK/ERK and PI3K pathways (8, and references therein), that lead to high VEGF levels and increased neo-angiogenesis. On the other hand, overexpression of c-mos regulates negatively the growth factor–dependent signaling cascades diminishing VEGF expression and tumor vascularization (42) **(C)**.

signal cascades (6–8). The fact that VEGF levels were almost similar in the group of K-ras(A)/c-mos(N) and that of K-ras(No)/c-mos(N) tumors, could be attributed, respectively, either to ras oncogenic activation or to ras activation by a variety of tumor growth factors that stimulate VEGF expression, such as epidermal growth factor (EGF), TGF-α, TGF-β, and PDGF, involved in autocrine growth loops in NSCL carcinogenesis (5,40). In these cases activated signaling cascades, such as MEK/ERK and PI3K pathways (8, and references therein), lead to high VEGF levels and increased neo-angiogenesis. On the other hand, c-mos might be involved in negative regulation of these growth factor–dependent cascades. In support of that, Faller et al. (41) showed that the PDGF autocrine growth stimulatory loop was functionally inhibited by v-mos.

In conclusion, our analysis suggests that c-mos may act as a molecular "switch" determining the effects of the growth factors/MEK/ERK pathway on NSCLC neo-angiogenesis (Fig. 7).

References

1. Folkman J. (1990). What is the evidence that tumors are angiogenesis dependent; *J. Natl. Cancer Inst.* **82:** 4–8.
2. Hanahan D, Folkman J. (1996). Patterns and emerging mechanisms of the angiogenic switch during tumorigenesis. *Cell* **86:** 353–364.
3. Bussolino F, Mantovani A, Persico G. (1997). Molecular mechanisms of blood vessel formation. *Trends Biochem. Sci.* **22:** 251–256.
4. Yancopoulos GD, Davis S, Gale NW, Rudge JS, Wiegand SJ, Holash J. (2000). Vascular-specific growth factors and blood vessel formation. *Nature* **407:** 242–248.
5. Dvorak HF, Brown LF, Detmar M, Dvorak AM. (1995). Vascular permeability factor/vascular endothelial growth factor, microvascular hypermeability and angiogenesis. *Am. J. Pathol.* **146:** 1029–1039.
6. Mukhopadhyay D, Tsiokas L, Zhou X-M, Foster D, Brugge JS, Sukhatme VP. (1995). Hypoxia induction of human vascular endothelial growth factor expression through c-Src activation. *Nature* **375:** 577–581.
7. Grugel S, Finkenzeller G, Weindel K, Barleon B, Marme D. (1995). Both v-Ha-ras and v-raf stimulate expression of the vascular endothelial growth factor in NIH3T3 cells. *J. Biol. Chem.* **270:** 25915–25919.
8. Rak J, Mitsuhashi Y, Sheehan C, et al. (2000). Oncogenes and tumor angiogenesis: differential modes of vascular endothelial growth factor up-regulation in ras-transformed epithelial cells and fibroblasts. *Cancer Res.* **60:** 490–498.
9. Crespo P, Leon J. (2000). Ras proteins in the control of the cell cycle and cell differentiation. *Cell. Mol. Life Sci.* **57:** 1613– 1636.
10. Moodie SA, Willumsem BM, Weber MJ, Wolfman A. (1993). Complexes of Ras. GTP with Raf and mitogen-activated protein kinase kinase. *Science* **260:** 1658–1661.
11. Schaeffer HJ, Weber MJ. (1999). Mitogen-activated protein kinases: specific messages from ubiquitous messengers. *Mol. Cell. Biol.* **19:** 2435–2444.
12. Rodriquez-Viciana P, Warne PH, Dhand R, et al. (1994). Phosphatydilinositol 3-kinase as a direct target for Ras. *Nature* **370:** 527–532.
13. Urano T, Emkey R, Feig LA. (1996). Ral GTPase mediate a distinct pathway from Ras that facilitates cellular transformation. *EMBO J.* **15:** 810–816.
14. Carnero A, Guadrado A, Peso L del, Lacal JC. (1994). Activation of type D phospholipase by serum stimulation and ras-induced transformation in NIH-3T3 cells. *Oncogene* **9:** 1387–1395.
15. Bos JL. (1998). A target for phosphoinositide 3-kinase: Akt/PKB. *Trends Biochem. Sci.* **20:** 441–442.
16. Whitmarsh A, Davis RJ. (1996). Transcription factor AP-1 regulation by mitogen-activated protein kinase signal transduction pathways. *J. Mol. Med.* **74:** 589–607.
17. Treisman R. (1996). Regulation of transcription by MAP kinase cascades. *Curr. Opin. Cell Biol.* **8:** 205–216.
18. Robinson MJ, Cobb MH. (1997). Mitogen-activated protein kinase pathways. *Curr. Opin. Cell Biol.* **9:** 180–186.
19. Okazaki M, Kisida S, Hinoi T, et al. (1997). Synergistic activation of c-fos promoter activity by Raf and Ral GDP dissociation stimulator. *Oncogene* **14:** 515–521.
20. Lowy DR, Willumsem BM. (1993). Function and regulation of ras. *Annu. Rev. Biochem.* **62:** 851–891.
21. Posada J, Yew N, Ahn NJ, vande Woude GF, Cooper JA. (1993). Mos stimulates MAP kinase in Xenopus oocytes and activates a MAP kinase kinase in vitro. *Mol. Cell Biol.* **13:** 2446–2453.
22. Sagata N. (1997). What does Mos do in oocytes and somatic cells? *BioEssays* **19:** 13–21.
23. Li C-CH, Chen E, O'Connell CD, Longo DL. (1993). Detection of *c-mos* proto-oncogene expression in human cells. *Oncogene* **8:** 1685–1691.
24. Fukasawa K, Vande Woude GF. (1995). Mos overexpression in Swiss 3T3 cells induces meiotic-like alterations of the mitotic spindle. *Proc. Natl. Acad. Sci. U.S.A.* **92:** 3430–3434.
25. Kolch W. (2000). Meaningful relationships: the regulation of the Ras/Raf/MEK/ERK pathway by protein interactions *J. Biochem.* **351:** 289–305.
26. Okazaki K, Sagata N. (1995). The Mos/MAP kinase pathway stabilizes c-Fos by phosphorylation and augments its transforming activity in NIH 3T3 cells. *EMBO J.* **14:** 5048– 5059.
27. Rhodes N, Innes CL, Propst F, Paules RS. (1997). Serum starved v-mos-transformed cells are unable to appropriately downregulate cyclins and CDKs. *Oncogene* **14:** 3017–3027.
28. Afshari CA, Rhodes N, Paules RS, Mudryj M. (1997). Deregulation of specific E2F complexes by v-mos oncogene. *Oncogene* **14:** 3029–3038.
29. Konishi T, Huang CL, Adachi M, et al. (2000). The K-ras gene regulates vascular endothelial growth factor gene expression in non-small cell lung cancers. *Int. J. Oncol.* **16:** 501–511.
30. Tsao MS, Liu N, Nicklee T, Shepherd F, Viallet J. (1997). Angiogenesis correlates with vascular endothelial growth factor expression but not with Ki-ras oncogene activation in non-small cell lung carcinoma. *Clin. Cancer Res.* **3:** 1807–1814.

31. Gorgoulis VG, Zacharatos P, Mariatos G, et al. (2001). Deregulated expression of c-mos in non-small cell lung carcinomas (NSCLCs). Relationship with p53 status, genomic instability and tumor kinetics. *Cancer Res.* **61:** 538–549.
32. Athanasiou A, Gorgoulis VG, Zacharatos P, et al. (2000). C-mos immunoreactivity is an indicator of good prognosis in lung cancer. *Histopathology* **37:** 45–54.
33. Kotsinas A, Spandidos DA, Romanowski P, Wyllie AH. (1993). Relative expression of wild-type and activated *Ki-ras2* oncogene in colorectal carcinomas. *Int. J. Oncol.* **3:** 841–845.
34. Hanahan D, Weinberg RA. (2000). The hallmarks of cancer. *Cell* **100:** 57–70.
35. Hunter T. (1997). Oncoprotein networks. *Cell* **88:** 333–346.
36. Holash J, Wiegand SJ, Yancopoulos GD. (1999). New model of tumor angiogenesis: dynamic balance between vessel regression and growth mediated by angiopoietins and VEGF. *Oncogene* **18:** 5356–5362.
37. Gum R, Wang H, Lengyel E, Juarez J, Boyd D. (1997). Regulation of 92kDa type IV collagenase expression by the jun aminoterminal kinase- and the extracellular signal-regulated kinase-dependent signaling cascades. *Oncogene* **14:** 1481–1493.
38. Wasylyk C, Gutman A, Nicholson R, Wasylyk B. (1991). The c-Ets oncoprotein activates the stromelysin promoter through the same elements as several non-nuclear oncoproteins. *EMBO J.* **10:** 1127–1134.
39. Simon C, Juarez J, Nicolson GL, Boyd D. (1996). Effects of PD098059, a specific inhibitor of mitogen-activated protein kinase kinase, on urokinase expression and in vitro invasion. *Cancer Res.* **56:** 5369–5374.
40. Sekido Y, Fong KM, Minna JD. (1998). Progress in understanding the molecular pathogenesis of human lung cancer. *Biochim. Biophys. Acta* **1378:** F21–F59.
41. Faller DV, Mundschau LJ, Forman LW, Quinones MA. (1994). v-mos suppresses platelet-derived growth factor (PDGF) type-beta receptor autophosphorylation and inhibits PDGF-BB-mediated signal transduction. *J. Biol. Chem.* **269:** 5022–5029.